Environmental Science & Technology

Article

pubs.acs.org/est

Field Deployable Chemical Redox Probe for Quantitative Characterization of Carboxymethylcellulose Modified Nano Zerovalent Iron

Dimin Fan,[†] Shengwen Chen,[‡] Richard L. Johnson,[†] and Paul G. Tratnyek*[,†]

[†]Institute of Environmental Health, Oregon Health and Science University, 3181 SW Sam Jackson Park Road, Portland, Oregon 97239, United States

[‡]School of Environmental and Materials Engineering, Shanghai Second Polytechnic University (SSPU), Shanghai 201209, People's Republic of China

Supporting Information

ABSTRACT: Nano zerovalent iron synthesized with carboxymethylcelluose (CMC-nZVI) is among the leading formulations of nZVI currently used for in situ groundwater remediation. The main advantage of CMC-nZVI is that it forms stable suspensions, which are relatively mobile in porous media. Rapid contaminant reduction by CMC-nZVI is well documented, but the fate of the CMC-nZVI (including "aging" and "reductant demand") is not well characterized. Improved understanding of CMC-nZVI fate requires methods with greater specificity for Fe(0), less vulnerability to sampling/recovery artifacts, and more practical application in the field. These criteria can be met with a simple and specific colorimetric approach using indigo-5,5′-disulfonate (I2S) as a chemical redox probe (CRP). The measured stoichiometric ratio for reaction between I2S and nZVI is 1.45 ± 0.03, suggesting complete oxidation of nZVI to Fe(III) species. However, near pH 7, reduction of I2S is diagnostic for Fe(0), because aqueous Fe(II) reduces I2S much more slowly than Fe(0). At that pH, adding Fe(II) increased I2S reduction rates by Fe(0), consistent with depassivation of nZVI, but did not affect the stoichiometry. Using the I2S assay to quantify changes in the Fe(0) content of CMC-nZVI, the rate of Fe(0) oxidation by water was found to be orders of magnitude faster than previously reported values for other types of nZVI.

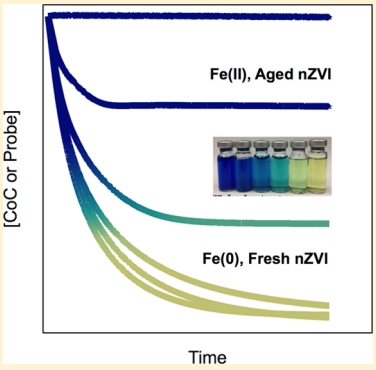

INTRODUCTION

Biogeochemical transformations of engineered nanomaterials (ENMs) significantly affect their fate, transport, and reactivity in the environment.[1−4] Nano zerovalent iron (nZVI) is unique among ENMs in that it is deliberately released into the environment under conditions that take advantage of its high reactivity for degradation of contaminants in groundwater.[5−8] However, the high reactivity of nZVI with contaminants also applies to reaction with other groundwater constituents and aquifer materials, resulting in substantial "reductant demand" in the short term,[9,10] "aging" in the medium term,[11−13] and stimulation/inhibition of various biogeochemical processes over the long-term.[14−17] For example, detailed studies of aging products formed from RNIP, one of the first commercial nZVI products used for remediation, showed significant loss of Fe(0) and formation of other iron mineral phases after one month exposure to anoxic water[11,18,19] and common groundwater constituents.[13] Using another commonly studied type of nZVI (synthesized with borohydride[20−22]), we showed that sulfidic groundwater conditions result in formation to iron sulfides, which changes the sequestration pathway for technetium.[23,24] However, these and most other studies of nZVI transformation (or aging) have been conducted in batch systems without the stabilizers used to make nZVI useful in field applications, which leaves considerable uncertainty regarding the transformation of stabilized formulations of nZVI under field conditions.

Many methods for improving the stability of nZVI suspensions have been investigated,[19,25−28] but one of the most widely used for field-scale groundwater remediation applications involves nZVI synthesized in the presence of carboxymethylcellulose (CMC).[9,27,29−32] Despite extensive characterization of the physical properties of CMC-nZVI, and its reactivity *with* contaminants, less is known about the chemical transformation *of* CMC-nZVI, especially after emplacement under field conditions. This is partly because the small size (~10 nm) and dispersion of the nZVI on the CMC polymer matrix results in stable solutions, from which the nZVI can not be recovered by conventional methods (filtration, centrifugation, etc.[33]). Without recovered solids, characterization of the nZVI using standard methods for nanomaterials (transmission electron microscopy, X-ray absorption spectroscopy, and X-ray diffraction[34]) is generally not feasible. Instead, characterization of the fate of CMC-nZVI, in both lab and field

Received: June 8, 2015
Revised: July 26, 2015
Accepted: July 28, 2015
Published: July 28, 2015

DOI: 10.1021/acs.est.5b02804
Environ. Sci. Technol. 2015, 49, 10589−10597

studies, has been based mainly on methods that provide bulk analyses of solution samples.

The bulk analyses that have been used to characterize CMC-nZVI include methods that respond directly to nZVI and those that are indirect in that they respond to the products of reaction between nZVI and the medium.[35] The *direct* methods include spectrophotometry at 800 nm (where Fe(0) should be the only species with significant absorbance)[9,35] or digestion followed by colorimetry for ferrozine complexed total iron.[35] *Indirect* methods that have been used to detect CMC-nZVI impacted fluids include measurement of changes in dissolved O_2, H_2, Fe(II), pH, and oxidation−reduction potential (ORP).[35,36] However, none of these bulk analysis methods are entirely specific for Fe(0), and the degree to which they are influenced by other reducing species (e.g., ferrous iron oxides and sulfides) is often uncertain. One assay that should be specific for Fe(0) involves acidification of samples and then measurement of H_2 from reduction of H^+, which has proven useful in laboratory[18] and field[31] studies, but aggressive digestion provides total Fe(0) and little information about the availability of that Fe(0) for reactions under environmentally relevant conditions. From a practical perspective, the most relevant way to characterize nZVI reactivity is by measuring the transformation kinetics and products of target (or model/probe) contaminants, but adding real contaminants for this purpose usually can only be done in laboratory studies and previously described "reactive tracer" compounds (e.g., trichlorofluoroethene, TCFE[37]) have not been evaluated for their behavior in ZVI containing systems.

In this study, we describe a simple, yet powerful, field-deployable method for characterizing nZVI reactivity and transformations using indigo-5,5′-disulfonate (I2S) as a reactive tracer or "chemical redox probe" (CRP). Although I2S and other redox active indicators have long been used in characterizing the redox properties of geochemical systems,[38−43] most of these studies have been focused on using indicator equilibrium to describe the thermodynamic conditions of the systems. In nZVI-containing systems, characterizing thermodynamic conditions is less useful because (i) the relevant species (Fe(0), Fe(II), Fe(III), H_2, etc.) are far from equilibrium with each other and (ii) any Fe(0) containing system has more than enough thermodynamic potential to affect the reduction of most contaminants. Instead, kinetic and capacity considerations are more relevant for characterizing nZVI exposed to media because these aspects are what controls the rate and extent of contaminant degradation. In the present study, we designed the experiments in such a way that I2S (which usually is used as a thermodynamic probe) serves mainly as a CRP for kinetic and capacity aspects of CMC-nZVI transformation and reactivity. The results suggest a practical method for characterizing nZVI that is deployable in the field as well as providing new insights into the factors that control the reactivity of nZVI in water.

EXPERIMENTAL SECTION

Chemical Reagents. All chemical regents except indigo-5,5′-disulfonate (indigo carmine, I2S) were ACS reagent grade and used as received without further purification. I2S was purchased from TCI America (Portland, OR), as the disodium salt, with 95% purity. Deoxygenated deionized (DO/DI) water was prepared by sparging with N_2 for 1 h and used to prepare deoxygenated stock solutions in an anoxic glovebox (100% N_2, O_2 < 0.8 ppm). A fresh CMC-nZVI suspension was prepared daily on the basis of the modified protocol adapted from He et al.,[26] which is detailed in the Supporting Information. The freshly prepared CMC-nZVI was determined to be 100% Fe(0) based on H_2 produced by acidification.[18]

CMC-nZVI Incubations. Several experimental variables, including CMC-nZVI concentration, pH, aging time, and the presence of Fe(II) and various anions, were chosen to simulate a range of conditions that are likely to result in transformation of CMC-nZVI during its transport in the subsurface. Accordingly, the stock CMC-nZVI suspension (1 g/L) was diluted to the target concentration with deoxygenated 10 mM HEPES at pH = 7.2 or 8.5 into 12 mL serum vials and crimp sealed with butyl rubber septa. The exposure time varied up to 24 h, which was chosen to cover the initial time period of rapid reactions after CMC-nZVI is first introduced into the subsurface (based on the results of the pilot injection we described in Johnson et al.[9]).

Probe Assay. At each sampling time, the incubated CMC-nZVI suspension was further diluted with DO/DI water to give 2−10 mg/L total iron with a final volume of 3.8 mL in a 1 cm cuvette. Dilution to low concentrations of nZVI was necessary to (i) give an initial rate of I2S reduction that is slow enough to measure accurately and (ii) make absorbance from CMC-nZVI negligible compared with I2S. The solution was buffered with 10 mM HEPES at pH 7.2 to avoid pH effects on probe reduction rate and absorptivity of the probe. The cuvette was sealed with a Viton-lined screw cap and then transferred out of the anaerobic chamber. Because the oxidized form of I2S has maximum absorbance wavelength (λ_{max}) at 610 nm (Figure S1), the initial absorbance at 610 nm contributed by CMC-nZVI (Abs_{ini}) was measured (PerkinElmer, Lambda 20 UV−vis spectrophotometer). Aliquots of ∼3.5 mM deoxygenated I2S stock solution (∼0.17 mL) were then injected into the cuvette through the septum to make an initial I2S concentration around 140 μM. The cuvette was mixed by hand for 5 s and placed into the UV−vis spectrophotometer. The decrease in absorbance at 610 nm (Abs_{610}) was continuously recorded as a function of time. After the reaction was complete, the solution was reoxidized by opening the cuvette, allowing ∼5 s exposure to ambient air, and then, absorbance (Abs_{reox}) was remeasured to determine the exact initial concentration of I2S in solution.

RESULTS AND DISCUSSION

Probe Properties. The oxidized quinoid form of I2S ($I2S_{ox}$) is bright blue (λ_{max} = 610 nm), and the reduced dihydro form ($I2S_{red}$) is pale yellow (λ_{max} = 407 nm) at circum-neutral pH.[38] At the concentrations used in this study (∼140 μM), the reduction of I2S is easily detected by the visible change of solution color from blue to yellow. We have shown previously that the sulfonated indigo redox indicators do not adsorb significantly to most relevant, environmental materials (ZVI, iron oxides, sediments, etc.)[38,44]

The overall half-reaction between $I2S_{ox}$ and $I2S_{red}$ (Scheme 1) has been studied thoroughly by potentiometric titration and

Scheme 1. Two-Electron Reduction Half-Reaction of Indigo-5,5′-disulfonate

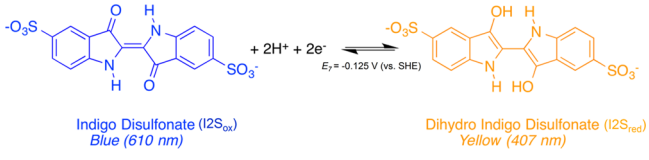

DOI: 10.1021/acs.est.5b02804
Environ. Sci. Technol. 2015, 49, 10589−10597

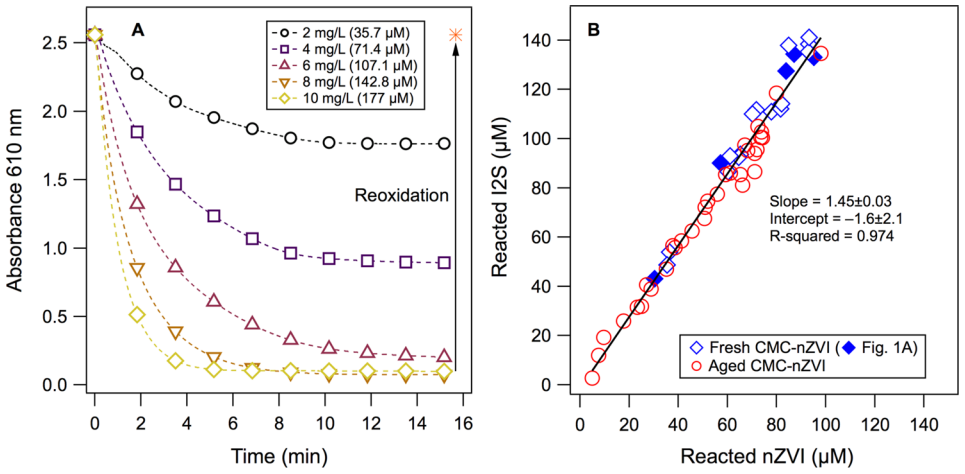

Figure 1. Determination of the apparent stoichiometry of the I2S reaction with nZVI: (A) Decrease in aqueous absorbance at 610 nm due to reduction of $I2S_{ox}$ by freshly prepared CMC-nZVI diluted to the specified initial concentrations. The asterisk represents Abs_{610} measured after sample reoxidation. (Data was recorded continuously, but markers are only shown every 1000 data points.) (B) Correlation between the amount of I2S reduction and nZVI oxidation for fresh and aged CMC-nZVI. (Each data point is derived from an individual I2S reduction curve, including the examples in A, shown by solid diamonds. The solid line corresponds to the linear regression coefficients given in the graph.)

found to give Nernstian response with a formal reduction potential of +0.291 V vs SHE at pH 0 (E_0') and −0.125 V at pH 7 (E_7).[45,46] The semiquinone intermediate is not expected to be significant below pH 9,[46] and no evidence (e.g., red color) for it was noted. $I2S_{red}$ has one environmentally relevant pK_a at 7.4 (for the first hydroxyl moiety),[38,46] but there is no acid−base speciation of $I2S_{ox}$ to affect its absorbance spectrum. The speciation of I2S is summarized in the Eh−pH diagram shown in Figure S1. Superimposing the most relevant stability fields for the iron system reveals that reduction of I2S by Fe(0) is thermodynamically favorable by >17 kcal at all pH's, whereas reduction by Fe(II) phases, such as Fe_3O_4, is only marginally favorable (~3 kcal) around neutral pH's.

Determining Apparent Stoichiometry. The half-reaction for the reduction of $I2S_{ox}$ to $I2S_{red}$ involves addition of two-electrons and two protons (Scheme 1). If Fe(II) is the end product of nZVI oxidation, then a 1-to-1 stoichiometric ratio between I2S reduced and CMC-nZVI oxidized is expected. To experimentally determine the reaction stoichiometry, we reduced ~140 μM $I2S_{ox}$ with freshly synthesized nZVI at concentrations ranging from 2 to 10 mg/L (defined by the total iron), corresponding to molar ratios of 0.25 to 1.25, and monitored the reaction by measuring Abs_{610}. The results (Figure 1A) show that the highest concentrations of nZVI (10 mg/L) gave a rapid decrease in absorbance, due to reduction of $I2S_{ox}$, followed by a well-defined plateau. At nZVI concentrations below 5 mg/L, the absorbance decreased more slowly and leveled out later at higher plateaus. The yellow color that developed in the aqueous phase of the high nZVI dose experiments indicates that there was complete reduction of $I2S_{ox}$ to $I2S_{red}$, and therefore, the plateau absorbance was due to excess nZVI. At lower nZVI doses (2 and 4 mg/L), the aqueous phase was still blue at the end of the experiments, indicating that $I2S_{ox}$ was in excess, which contributes to the absorbance plateau.

To calculate the concentrations of I2S and nZVI based on absorbance spectra shown in Figure 1A, four species that could contribute to Abs_{610} were considered, including $I2S_{ox}$, $I2S_{red}$, $nZVI_{red}$ (fully reduce material, as originally synthesized), and $nZVI_{ox}$ (fully oxidized material). The full absorbance spectra of individual species (Figure S2), obtained independently, but at relevant concentrations, show that $I2S_{ox}$ contributed >90% of Abs_{610}, $nZVI_{red}$ contributed less than 10%, and neither $I2S_{red}$ nor $nZVI_{ox}$ (obtained by exposing fresh CMC-nZVI to air) contribute significantly. Using a calibration curve for $I2S_{ox}$ obtained at 610 nm (Figure S3), the amount of I2S reduction was calculated from the difference in absorbance between of (i) the fully reoxidized sample (Abs_{reox}) and (ii) the final, plateau absorbance (Abs_{end}) if I2S was in excess or simply Abs_{reox} if nZVI was in excess. Likewise, using the calibration curve for nZVI (Figure S3), the amount of nZVI oxidation was determined from (i) the initial absorbance of the suspension before I2S addition (Abs_{ini}) if nZVI was completely oxidized or (ii) the difference between Abs_{ini} and Abs_{end} (because $I2S_{red}$ showed little absorbance at 610 nm) if nZVI was in excess. The majority of the experiments were conducted with $I2S_{ox}$ in excess because the larger absorptivity of $I2S_{ox}$ gave more reliable measurements.

Plotting the amount of I2S reduction against the amount of nZVI oxidation for all experiments (Figure 1B) shows that the quantities of reacted I2S and nZVI give a strong linear correlation, for both fresh and aged nZVI. Regression on the correlation in Figure 1B gives a slope of 1.45 ± 0.03, which is the experimental stoichiometry for reaction between I2S and nZVI, and is significantly greater than the 1:1 stoichiometry that would be expected if Fe(II) was the oxidation end point.

The "excess" stoichiometry was not due to loss of $I2S_{ox}$ by adsorption to nZVI surfaces because reoxidation of the aqueous suspension at the end of the experiments immediately gave complete recovery of the initial absorbance at 610 nm (Figure 1A, asterisk). Alternatively, the excess could be due to reactions with reductants other than nZVI, such as residual borohydride from nZVI synthesis, or Fe(II) species (aqueous or solid) generated from nZVI oxidation by $I2S_{ox}$. However, residual borohydride should be negligible because the synthesis was performed with borohydride and Fe(II) at concentrations that exactly match the expected 2:1 stoichiometry of the Fe(0) formation reaction.[47] Reduction of I2S by aqueous Fe(II) at pH 7.2 was excluded, as well, because control experiments with aqueous Fe(II) gave negligible I2S reduction (Figure S4). The remaining candidate is solid phase Fe(II), e.g., Fe(II) minerals or sorbed Fe(II), which has been shown (as stronger reductants

DOI: 10.1021/acs.est.5b02804
Environ. Sci. Technol. 2015, 49, 10589−10597

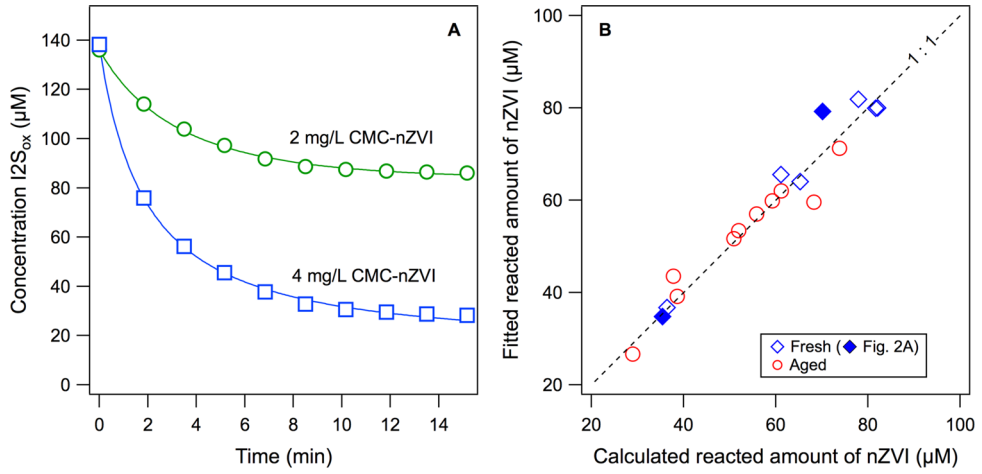

Figure 2. Second-order kinetic modeling: (A) Fitting of representative data for I2S reduction by freshly prepared CMC-nZVI diluted to 2 and 4 mg/L in pH 7.2 HEPES buffer (the concentration was calculated on the basis of the absorbance data shown in Figure 1A); (B) Correlation between oxidized nZVI determined by fitting and oxidized nZVI determined by absorbance.

than aqueous Fe(II)) to reduce a variety of organic compounds, including redox mediators that are analogous to I2S.[48,49] Complete oxidation of solid Fe(II) results in Fe(III) oxyhyroxide, which suggests the following overall reaction between Fe(0) and I2S$_{ox}$.

$$2Fe(0) + 3[I2S_{ox}] + 6H_2O \rightarrow 2Fe(III) + 3[I2S_{red}] + 6OH^- \quad (1)$$

Eq 1 suggests a stoichiometric ratio between I2S$_{ox}$ and Fe(0) of 1.5, which is consistent with the calculated ratio of 1.45 ± 0.03, obtained from Figure 1B.

Note that the calculated stoichiometry is slightly less than the theoretical value of 1.5. This difference could be due to the parallel reaction between nZVI and water (i.e., anaerobic corrosion). Control experiments to characterize the rate of this reaction were performed by measuring the decrease in Abs_{610} in DO/DI water, under the same conditions as the probe assay but without I2S. The results (Figure S5) show that, at pH 7.2, the reactions were slower compared to oxidation by I2S, but still caused 5—10% of Fe(0) loss over the time frame of the probe assay. The Fe(0) loss was less at pH 8.5, but Figure S4 showed appreciable I2S reduction by aqueous Fe(II) only at this pH. Therefore, conducting the I2S assay at high pH might overestimate the quantity of Fe(0), especially under field conditions, where significant Fe(II) is likely to be present as a result of Fe(0) corrosion. Although the rates of nZVI reaction with water in the presence of I2S$_{ox}$ might be different than those measured in Figure S5 due to competitive reaction with I2S$_{ox}$, these results are consistent with a stoichiometric ratio of 1.45, due to a small fraction of nZVI oxidation by H_2O rather than by I2S.

Fitting Second Order Kinetics. In all experiments reported in this study, neither nZVI nor I2S were in significant excess, so the requirement for application of pseudo first-order kinetics was not met.[50,51] Instead, the data were fit to a second order kinetic model adapted from a previous study on a system with some similar characteristics: reduction of lepidocrocite by reduced anthraquinone disulfonate (AH_2DS).[52] To implement this model, several simplifying assumptions were made: (i) Fe(0) and all Fe(II)-containing solid phases were modeled as a single reducing species, and (ii) the reaction rate was first order with respect to the individual reactants nZVI and I2S. The reaction rate (r) for eq 1 is given by eq 2:

$$r = \frac{d[I2S_{ox}]}{dt} = k''[I2S_{ox}][nZVI_{red}] \quad (2)$$

where [I2S$_{ox}$] is the concentration of oxidized I2S (μM), k'' is the second-order reaction rate constant (μM^{-1} min^{-1}), and [nZVI] is the concentration of nZVI. Solving eq 2 for of I2S$_{ox}$ versus time (following the treatment by Shi et al.[52]) gave eq 3:

$$[I2S_{ox}]_t = [I2S_{ox}]_0 - \frac{1.5 \times [I2S_{ox}] \times [nZVI_{red}]_0 \times (e^{[nZVI]_0 kt} - e^{2/3[I2S_{ox}]_0 kt})}{1.5 \times [nZVI_{red}]_0 \times e^{[nZVI]_0 kt} - [I2S_{ox}] \times e^{2/3[I2S_{ox}]kt}} \quad (3)$$

where [I2S$_{ox}$]$_0$ is the initial I2S$_{ox}$ concentration, [nZVI]$_0$ is the initial nZVI concentration, and k'' is the second order reaction constant. The latter two parameters were determined by fitting eq 3 to [I2S$_{ox}$] vs time data.

As can be seen from the examples in Figure 2A, this approach fit the data very well, indicating that the second-order kinetic model eq 2 is appropriate for describing the kinetics of I2S reduction by CMC-nZVI under the conditions of this study. At relatively high nZVI/I2S ratios, a small but consistent degree of tailing was observed (e.g., 4 mg/L in Figure 2A), which may be due to (i) small contributions of nZVI (<5%) to the overall absorbance (cf. Figure S2), which was not included when calculating I2S concentrations, or (ii) the inclusion of solid Fe(II) with Fe(0) in the term for [nZVI], which would not fully describe the I2S reduction kinetics if there was substantial variations in the contributions of Fe(0) and solid Fe(II). The model was fit only to the data where nZVI was completely consumed (2 and 4 mg/L total iron) because the quantity of I2S reduction can be more accurately determined than the amount of nZVI oxidation (due to high absorptivity of I2S$_{ox}$, as noted above).

Another way to examine the kinetic modeling results is to compare the molar concentration of oxidized nZVI obtained from the fit to eq 3 against those calculated from the Abs_{610} measured before addition of I2S. The resulting correlation shown in Figure 2B (for all the conditions tested, not just the examples shown in Figure 2A) suggests good agreement between fitted and measured values for reacted nZVI as all the

DOI: 10.1021/acs.est.5b02804
Environ. Sci. Technol. 2015, 49, 10589−10597

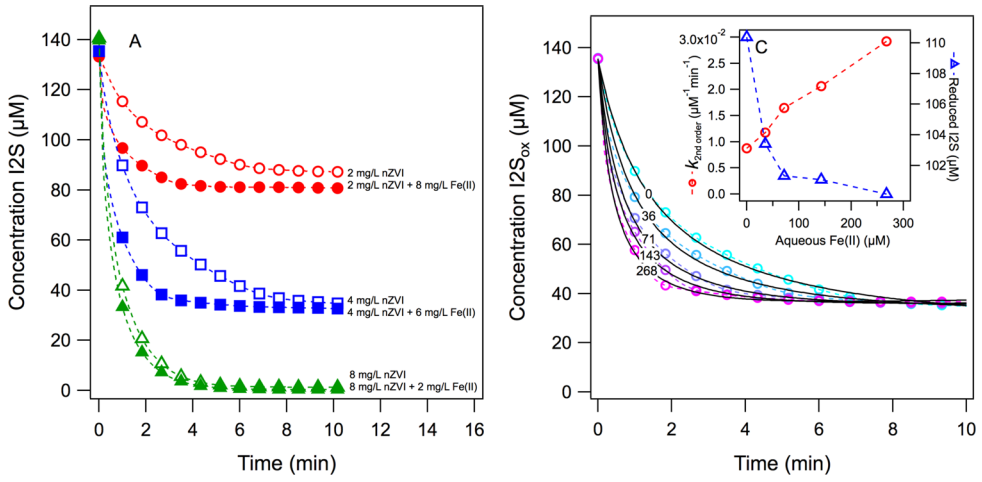

Figure 3. Effect of Fe(II) on I2S reduction by Fe(0): (A) I2S reduction by mixtures of Fe(II) and nZVI with the total iron concentration of 10 mg/L and equal concentrations of nZVI without Fe(II). (B) I2S reduction by 4 mg/L nZVI with aqueous Fe(II) concentrations from 0 to 15 mg/L (open symbols are experimental data, and solid lines are second-order kinetic fits). (C) Second-order rate constant (left axis) and amount of I2S reduction (right axis) extracted from fitting the data in (B).

data points follow the 1:1 line with no bias and little scatter. Similar to Figure 1B, both fresh and aged samples were well described (Figure 2B), demonstrating that the model is sufficiently robust to be used in characterization of the range of subsurface media conditions created by the impacts of nZVI emplacement.

Distinguishing Fe(II) from Fe(0). The negligible rate of I2S reduction by aqueous Fe(II) alone at pH 7.2 (Figure S4) suggests that I2S could be useful as a CRP to distinguish aqueous Fe(II) from Fe(0), such as to quantify the Fe(0) (as opposed to total iron) in groundwater samples used to characterize the distribution of nZVI after injection into the subsurface. Because aqueous Fe(II) would coexist with Fe(0) in the field, we measured the rates of I2S reduction in mixtures of aqueous Fe(II) and CMC-nZVI, with Fe(0)/Fe(II) ratio varied from 0.25 to 4, but constant 10 mg/L total iron, at pH 7.2. These data are shown in Figure 3A, together with data for the corresponding nZVI dose without added Fe(II). With and without added Fe(II), the higher Fe(0) concentrations gave more complete reduction of I2S (similar to the results seen in Figures 1A and 2A). The primary effect of added Fe(II) was to increase the rate at which the limiting I2S concentration was reached, but the Fe(II) does not appear to provide additional capacity for I2S reduction (because the limiting $I2S_{ox}$ concentrations are nearly the same with and without added Fe(II)). The quantity of I2S reduced at the plateau values is approximately 1.5 times the amount of nZVI oxidation in these experiments, which is consistent with the reaction stoichiometry determined above, eq 1, and further evidence that aqueous Fe(II) is not directly responsible for reduction of I2S.

The increased rate of I2S reduction caused by addition of Fe(II) to CMC-nZVI (shown in Figure 3A) was further investigated at 4 mg/L nZVI by systematically varying added Fe(II) from 0 to 15 mg/L (0–268 μm) (Figure 3B). The data were again fitted using eq 3, and the resulting rate constants (k'') are plotted against aqueous Fe(II) in Figure 3C (left axis). Increasing aqueous Fe(II) produced a monotonic, and nearly linear, increase in k'', whereas the plateau concentration of I2S decreased nonlinearly with Fe(II) (right axis in Figure 3C). The difference between the two trends in Figure 3C could be because Fe(II) increases the rate of nZVI reaction with water as well, resulting in less Fe(0) to reduce I2S. This effect would be consistent with several recent studies that have concluded that adsorption of Fe(II) to the oxide film on Fe(0) results in depassivation, accelerated corrosion of Fe(0), and concomitant enhancment of the reduction rate of target contaminants.[53,54] Under the strictly anoxic conditions of this study, there should be little if any Fe(III) oxide on the unreacted nZVI. This suggests that the effect of aqueous Fe(II) on rates of probe/contaminant reduction might apply in nonaged (n)ZVI systems as well any system where the ZVI is passivated by significant qauntities of Fe(III) oxides.

Quantifying the Lifetime of nZVI in Water. An extension and application of using I2S as a CRP is for the quantification of nZVI transformation in the presence of background "reductant demand" (i.e., oxidation by reaction with water). Previous studies that have addressed this issue have relied mainly on measurement of H_2 that is formed from acid digestion of Fe(0). This assay has been performed by measuring the volume or pressure of H_2 gas produced[55,56] or concentration of dissolved H_2 by gas chromatography,[18,57] but the former requires large sample volumes and has low sensitivity and the latter requires special sample handling and relatively-specialized instrumentation. Even more specialized methods of determining Fe(0) include fitting of XRD and Mössbauer data.[11,19,58] In contrast, reduction of I2S provides an assay that is selective for Fe(0), requires only small sample volumes (<1 mL), provides immediate results, and can easily be implemented in the field.

To test the applicability of I2S for quantifying Fe(0) reaction with water, the I2S assay was applied to determine molar Fe(0) content (i.e., $Fe(0)/Fe_{total}$[11,19]) as a function of time on CMC-nZVI suspensions with a range of initial nZVI concentrations and pH's (chosen to represent the degree of nZVI dilution[9] and range of pH[59] that have been observed during injection and transport of CMC-nZVI in the field). The initial portion of the resulting data (Figure 4) was fit by pseudo-first order kinetics, giving k_{obs} values ranging from 0.02 to 0.26 h^{-1} ($t_{1/2} \approx 3$–33 h). These rate constants are 2–3 orders of magnitude greater than previously reported rates for several conventional types of nZVI (determined by measuring H_2 evolution), which include 6×10^{-3} d^{-1} for RNIP[18] and 2.72×10^{-2} d^{-1} for NANOFER[58]

DOI: 10.1021/acs.est.5b02804
Environ. Sci. Technol. 2015, 49, 10589–10597

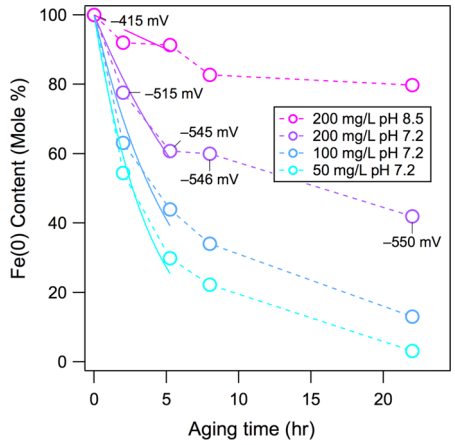

Figure 4. Quantifying the lifetime of nZVI in DO/DI water: Kinetics of Fe(0) oxidation by water with 50, 100, and 200 mg/L initial nZVI concentrations (in 10 mM HEPES buffer at pH 7.2) and 200 mg/L initial nZVI concentration (in 10 mM HEPES buffer of pH 8.5). Each data point was determined by I2S reduction in subsamples of the nZVI suspension. Labels are ORP measured with a Pt electrode and reported vs SHE.

(another widely used formulation of commercially available nZVI). The reaction rate of background reductant demand with CMC-nZVI is expected to be greater than other types of nZVI, because of the smaller size and greater dispersion of the primary particles in CMC-nZVI (Figure S8), but the large degree to which this process is accelerated with CMC-nZVI is another way (in addition to forming true solutions) in which this material is qualitatively different than the other Fe(0)-based reductants that are widely used.

The half-lives that correspond to the kinetics shown in Figure 4 are on the order of hours, which matches the time frame of typical laboratory column or field transport studies of nZVI. In most of these studies, the implications of Fe(0) oxidation by reaction with water, although occasionally reported,[59] are not fully evaluated. The results presented here suggest that the decrease in Fe(0) content of CMC-nZVI may be great enough to influence the kinetics of contaminant degradation measured in batch experiments with contaminants such as the chlorinated ethenes (TCE, etc.) because they react more slowly than water with CMC-nZVI. Over longer time periods, such as during full-scale field applications, the conversion of Fe(0) to Fe(II) by background reductant demand processes is certain to have a large effect on net rates of contaminant reduction (given that most contaminants are reduced much more rapidly by Fe(0) than Fe(II) in any form).[60,61] Therefore, characterization of nZVI delivery in field applications should be based mainly on assays that can distinguish Fe(0) from other iron species, and this could be done efficiently with the I2S assay described here.

The results (Figure 4) show that the rate of Fe(0) loss (normalized to the initial nZVI dose), due to reductant demand from reaction with water, is mostly affected by two parameters that vary significantly under field conditions: pH and the concentration of nZVI (except for phosphate, adding 0.5 mM of various anions had minimal effects (Figure S7)). The data in Figure 4 suggests that the Fe(0) loss rate was greatest at lower initial Fe(0) concentrations, which implies that the dilution of nZVI (e.g., downgradient from an injection point) will cause the reaction rate with reductant demand to increase. Note that the concentrations used in prior studies on nZVI dissolution rates were at least one order of magnitude higher than the concentrations tested here, which are more representative of the field conditions. Therefore, actual dissolution rates under field conditions might be higher than expected based on previous laboratory results.

With respect to pH, for 200 mg/L CMC-nZVI, Fe(0) loss was significantly slower at pH 8.5 than at 7.2. Loss of Fe(0) was also relatively slow in the freshly prepared CMC-nZVI suspension (without dilution in HEPES buffer), which had high concentration (1 g/L) and high pH, and for 200 mg/L nZVI aged in DO/DI water without buffer (Figure S6). It is worth noting that, for the latter experiment, initial Fe(0) loss was still fast (slope similar to 200 mg/L nZVI in pH 7.2 buffer) but tailing becomes evident after about 5 h, possibly due to the increase in pH (up to ~9) driven by reaction of Fe(0) with water. These results are consistent with a previous study that showed H_2 production for RNIP was inhibited at high pH.[18] In that study, the formation of iron oxides (such as Fe_3O_4 or green rust) was invoked as a potential explanation for suppressing H_2 production. While Fe_3O_4 formation was plausible (e.g., by the Shickorr reaction[58]), it is not certain that the same mechanism applies under the conditions of this study. One argument against significant passivation of CMC-nZVI by coating Fe(0) with Fe_3O_4 is that reduction of I2S dominated by Fe_3O_4 should produce a stoichiometry of 1:2 (based on electron equivalence calculations similar to those described), but the observed I2S/Fe(0) stoichiometric ratio remained about 1.4 throughout the experiments shown in Figure 4 (data not shown). Nevertheless, the possibility of forming a thin/conductive layer of Fe_3O_4, which might not affect the apparent overall stoichiometry, cannot be excluded. Detailed characterization of surface layer mineralogy would be needed to address this issue, but only the TEM given in Figure S8 was performed as part of this study.

Oxidation reduction potential (ORP) was measured using a combination (Pt) ORP electrode on the samples from the experiment with 200 mg/L nZVI at pH 7.2. The results, given as annotations in Figure 4, show that the ORP became more negative as Fe(0) content decreased (due to reaction with water). This trend is opposite to the relationship between ORP and Fe(0) that is commonly assumed when ORP is used as an indicator for nZVI in studies of emplacement and transport.[35] However, several effects that complicate the interpretation of ORP measurement in the presence of nZVI have been identified,[35,36] and the ORP data in Figure 4 apparently reflect those effects. For example, the sensitivity of Pt ORP electrodes to dissolved H_2 probably explains why the measured ORP decreased from −415 to −550 mV during the first 2 h, whereas the Fe(0) content (determined by the I2S assay) decreased 20%. Later, the decrease in measured ORP appears to have leveled out to a greater degree than the decrease in Fe(0) content, which again is consistent with the Nernstian response of the Pt electrode in a system that is accumulating high contentrations of H_2. These complications in interpretation of the ORP data are further evidence for why ORP measured with a conventional Pt electrode is not a straightforward indicator of the presence of nZVI and probably only should be used in conjuction with complementary methods[35] including I2S as a CRP for Fe(0).

Implications for Field Applications and nZVI Improvement. The selectivity of I2S for Fe(0) could make this assay especially beneficial for field applications of nZVI, where the abundance of coexisting redox active species and complex water chemistry greatly complicates the ability of conventional

DOI: 10.1021/acs.est.5b02804
Environ. Sci. Technol. 2015, 49, 10589−10597

methods (e.g., ORP) to detect Fe(0) impacted zones. A simple and robust protocol for field deployment would be to inject a known volume of water sample containing nZVI into a deoxygenated and buffered solution with known concentration of I2S in a sealed vial (prepared in advance in the laboratory). After injection, the absorbance change at 610 nm can easily be recorded over time with a portable spectrophotometer. The concentration range of nZVI should be diluted to less than half of the initial I2S concentration used, to ensure complete consumption of nZVI (based on the stoichiometric ratio of reaction between nZVI and I2S calculated from Figure 1B). The required dilution factor can be predetermined by estimating the nZVI concentration in the water samples with a total iron or absorbance measurement. Although measuring the initial absorbance of the nZVI suspension without I2S can be used in quantifying nZVI concentration in the laboratory (Figure S2), it will likely be less reliable in field applications because of interference from background turbidity or absorbance in natural groundwater samples. The CRP approach, on the other hand, is not subject to interference by background absorbance because the change in absorbance is used for calculating nZVI concentration.

Current field scale applications of nZVI are limited primarily by two factors: transport and longevity. Many approaches have been proposed to overcome the transport or longevity limitations of nZVI, but many solutions for one limitation are contradictory to solutions to the other limitation. These contradictions are especially evident for CMC-nZVI, which has enhanced mobility but orders of magnitude shorter lifetime in groundwater than most other types of nZVI. Refining nZVI formulation to achieve balance between these two aspects should be the focus of the next phase of nZVI development. During this process, the reactions with I2S (and potentially other CRPs) could serve as an easy and quick assay to more efficiently evaluate the reactive transformations of nZVI and their effects on nZVI lifetime and provide guidance on improved design of nZVI to achieve field applicability. In addition, data on the rates of probe compound reduction might facilitate "higher order" use of CRP data, such as developing correlations with the relatively slow kinetics of contaminant reduction to allow rapid screening of the reactivity of nZVI to target contaminants.

■ ASSOCIATED CONTENT

Supporting Information

The Supporting Information is available free of charge on the ACS Publications website at DOI: 10.1021/acs.est.5b02804.

Details on absorbance calibrations of I2S and CMC-nZVI, parallel nZVI dissolution during probe reaction, I2S reduction by aqueous Fe(II), and nZVI dissolution kinetics in original synthesis solution and in DO/DI water at 200 mg/L (PDF)

■ AUTHOR INFORMATION

Corresponding Author

*E-mail: tratnyek@ohsu.edu; phone: 503-346-3431; fax: 503-346-3427.

Notes

The authors declare no competing financial interest.

■ ACKNOWLEDGMENTS

This material is based on work supported by the Strategic Environmental Research and Development Program of the U.S. Department of Defense, Award Number ER-2308. The authors would like to thank Andrew Barnum at Portland State University for collecting the transmission electron micrographs.

■ REFERENCES

(1) Nowack, B.; Ranville, J. F.; Diamond, S.; Gallego-Urrea, J. A.; Metcalfe, C.; Rose, J.; Horne, N.; Koelmans, A. A.; Klaine, S. J. Potential scenarios for nanomaterial release and subsequent alteration in the environment. *Environ. Toxicol. Chem.* **2012**, *31*, 50−59.

(2) Lowry, G. V.; Gregory, K. B.; Apte, S. C.; Lead, J. R. Transformations of nanomaterials in the environment. *Environ. Sci. Technol.* **2012**, *46*, 6893−6899.

(3) Maynard, A. D.; Aitken, R. J.; Butz, T.; Colvin, V.; Donaldson, K.; Oberdorster, G.; Philbert, M. A.; Ryan, J.; Seaton, A.; Stone, V.; Tinkle, S. S.; Tran, L.; Walker, N. J.; Warheit, D. B. Safe handling of nanotechnology. *Nature* **2006**, *444*, 267−269.

(4) Wagner, S.; Gondikas, A.; Neubauer, E.; Hofmann, T.; von der Kammer, F. Spot the difference: Engineered and natural nanoparticles in the environment - Release, behavior, and fate. *Angew. Chem., Int. Ed.* **2014**, *53*, 12398−12419.

(5) Tosco, T.; Petrangeli Papini, M.; Cruz Viggi, C.; Sethi, R. Nanoscale zerovalent iron particles for groundwater remediation: A review. *J. Cleaner Prod.* **2014**, *77*, 10−21.

(6) Crane, R. A.; Scott, T. B. Nanoscale zero-valent iron: Future prospects for an emerging water treatment technology. *J. Hazard. Mater.* **2012**, *211−212*, 112−125.

(7) Yan, W.; Lien, H.-L.; Koel, B. E.; Zhang, W.-X. Iron nanoparticles for environmental clean-up: Recent developments and future outlook. *Environ. Sci.: Processes Impacts* **2013**, *15*, 63−77.

(8) O'Carroll, D.; Sleep, B.; Krol, M.; Boparai, H.; Kocur, C. Nanoscale zero valent iron and bimetallic particles for contaminated site remediation. *Adv. Water Resour.* **2013**, *51*, 104−122.

(9) Johnson, R. L.; Nurmi, J. T.; O'Brien Johnson, G.; Fan, D.; O'Brien Johnson, R.; Shi, Z.; Salter-Blanc Alexandra, J.; Tratnyek, P. G.; Lowry, G. V. Field-scale transport and transformation of carboxymethylcellulose-stabilized nano zero-valent iron. *Environ. Sci. Technol.* **2013**, *47*, 1573−1580.

(10) Tratnyek, P. G.; Johnson, R. L.; Lowry Gregory, V.; Brown, R. A. In situ chemical reduction for source zone remediation. In *Chlorinated Solvent Source Zone Remediation*; Kueper, B. H.; Stroo, H. F.; Vogel, C. M.; Ward, C. H., Eds.; Springer: New York, 2014; SERDP and ESTCP Remediation Technology Monograph Series, Vol. 7; pp 307−351.

(11) Sarathy, V.; Tratnyek, P. G.; Nurmi, J. T.; Baer, D. R.; Amonette, J. E.; Chun, C.; Penn, R. L.; Reardon, E. J. Aging of iron nanoparticles in aqueous solution: effects on structure and reactivity. *J. Phys. Chem. C* **2008**, *112*, 2286−2293.

(12) Phenrat, T.; Long, T. C.; Lowry, G. V.; Veronesi, B. Partial oxidation ("aging") and surface modification decrease the toxicity of nanosized zerovalent iron. *Environ. Sci. Technol.* **2009**, *43*, 195−200.

(13) Reinsch, B. C.; Forsberg, B.; Penn, R. L.; Kim, C. S.; Lowry, G. V. Chemical transformations during aging of zerovalent iron nanoparticles in the presence of common groundwater dissolved constituents. *Environ. Sci. Technol.* **2010**, *44*, 3455−3461.

(14) Kumar, N.; Omoregie, E. O.; Rose, J.; Masion, A.; Lloyd, J. R.; Diels, L.; Bastiaens, L. Inhibition of sulfate reducing bacteria in aquifer sediment by iron nanoparticles. *Water Res.* **2014**, *51*, 64−72.

(15) Bruton, T. A.; Pycke, B. F. G.; Halden, R. U. Effect of nanoscale zero-valent iron treatment on biological reductive dechlorination: A review of current understanding and research needs. *Crit. Rev. Environ. Sci. Technol.* **2015**, *45*, 1148−1175.

(16) Fajardo, C.; Ortíz, L. T.; Rodríguez-Membibre, M. L.; Nande, M.; Lobo, M. C.; Martin, M. Assessing the impact of zero-valent iron (ZVI) nanotechnology on soil microbial structure and functionality: A molecular approach. *Chemosphere* **2012**, *86*, 802−808.

(17) Němeček, J.; Lhotský, O.; Cajthaml, T. Nanoscale zero-valent iron application for in situ reduction of hexavalent chromium and its effects on indigenous microorganism populations. *Sci. Total Environ.* **2014**, *485−486*, 739−747.
(18) Liu, Y.; Lowry, G. V. Effect of particle age (Fe^0 content) and solution pH on nZVI reactivity: H_2 evolution and TCE dechlorination. *Environ. Sci. Technol.* **2006**, *40*, 6085−6090.
(19) Tratnyek, P. G.; Salter-Blanc, A. J.; Nurmi, J. T.; Amonette, J. E.; Liu, J.; Wang, C.; Dohnalkova, A.; Baer, D. R. Reactivity of zerovalent metals in aquatic media: Effects of organic surface coatings. In *Aquatic Redox Chemistry*; Tratnyek, P. G., Grundl, T. J., Haderlein, S. B., Eds.; American Chemical Society: Washington, DC, 2011; ACS Symposium Series, Vol. *1071*; pp 381−406.
(20) Liu, A.; Liu, J.; Zhang, W.-X. Transformation and composition evolution of nanoscale zero valent iron (nZVI) synthesized by borohydride reduction in static water. *Chemosphere* **2015**, *119*, 1068−1074.
(21) Woo, H.; Park, J.; Lee, S.; Lee, S. Effects of washing solution and drying condition on reactivity of nano-scale zero valent irons (nZVIs) synthesized by borohydride reduction. *Chemosphere* **2014**, *97*, 146−152.
(22) Sun, Q.; Feitz, A. J.; Guan, J.; Waite, T. D. Comparison of the reactivity of nanosized zero-valent iron (nZVI) particles produced by borohydride and dithionite reduction of iron salts. *Nano* **2008**, *3*, 341−349.
(23) Fan, D.; Anitori, R. P.; Tebo, B. M.; Tratnyek, P. G.; Lezama Pacheco, J. S.; Kukkadapu, R. K.; Engelhard, M. H.; Bowden, M. E.; Kovarik, L.; Arey, B. W. Reductive sequestration of pertechnetate ($^{99}TcO_4^-$) by nano zero-valent iron (nZVI) transformed by abiotic sulfide. *Environ. Sci. Technol.* **2013**, *47*, 5302−5310.
(24) Fan, D.; Anitori, R. P.; Tebo, B. M.; Tratnyek, P. G.; Lezama Pacheco, J. S.; Kukkadapu, R. K.; Kovarik, L.; Engelhard, M. H.; Bowden, M. E. Oxidative remobilization of technetium sequestered by sulfide-transformed nano zerovalent iron. *Environ. Sci. Technol.* **2014**, *48*, 7409−7417.
(25) Johnson, R. L.; O'Brien Johnson, R.; Nurmi, J. T.; Tratnyek, P. G. Natural organic matter enhanced mobility of nano zero-valent iron. *Environ. Sci. Technol.* **2009**, *43*, 5455−5460.
(26) He, F.; Zhao, D. Manipulating the size and dispersibility of zerovalent iron nanoparticles by use of carboxymethyl cellulose stabilizers. *Environ. Sci. Technol.* **2007**, *41*, 6216−6221.
(27) Busch, J.; Meißner, T.; Potthoff, A.; Bleyl, S.; Georgi, A.; Mackenzie, K.; Trabitzsch, R.; Werban, U.; Oswald, S. E. A field investigation on transport of carbon-supported nanoscale zero-valent iron (nZVI) in groundwater. *J. Contam. Hydrol.* **2015**, in press; DOI: 10.1016/j.jconhyd.2015.03.009.
(28) Saleh, N.; Sirk, K.; Liu, Y.; Phenrat, T.; Dufour, B.; Matyjaszewski, K.; Tilton, R. D.; Lowry, G. V. Surface modifications enhance nanoiron transport and NAPL targeting in saturated porous media. *Environ. Eng. Sci.* **2007**, *24*, 45−57.
(29) He, F.; Zhang, M.; Qian, T.; Zhao, D. Transport of carboxymethyl cellulose stabilized iron nanoparticles in porous media: Column experiments and modeling. *J. Colloid Interface Sci.* **2009**, *334*, 96−102.
(30) He, F.; Zhao, D.; Paul, C. Field assessment of carboxymethyl cellulose stabilized iron nanoparticles for in situ destruction of chlorinated solvents in source zones. *Water Res.* **2010**, *44*, 2360−2370.
(31) Kocur, C. M.; O'Carroll, D. M.; Sleep, B. E. Impact of nZVI stability on mobility in porous media. *J. Contam. Hydrol.* **2013**, *145*, 17−25.
(32) Krol, M. M.; Oleniuk, A. J.; Kocur, C. M.; Sleep, B. E.; Bennett, P.; Xiong, Z.; O'Carroll, D. M. A field-validated model for in situ transport of polymer-stabilized nZVI and implications for subsurface injection. *Environ. Sci. Technol.* **2013**, *47*, 7332−7340.
(33) Nurmi, J. T.; Sarathy, V.; Tratnyek, P. G.; Baer, D. R.; Amonette, J. E.; Linehan, J. C.; Karkamkar, A. Recovery of iron/iron oxide nanoparticles from aqueous media: A comparison of methods and their effects. *J. Nanopart. Res.* **2011**, *13*, 1937−1952.
(34) Baer, D. R.; Tratnyek, P. G.; Qiang, Y.; Amonette, J. E.; Linehan, J.; Sarathy, V.; Nurmi, J. T.; Wang, C.; Antony, J. Synthesis, characterization, and properties of zero-valent iron nanoparticles. In *Environmental Applications of Nanomaterials*, 2nd ed.; Imperial College Press: London, 2012; pp 49−86.
(35) Shi, Z.; Fan, D.; Johnson, R. L.; Tratnyek, P. G.; Nurmi, J. T.; Wu, Y.; Williams, K. H. Methods for characterizing the fate and effects of nano zerovalent iron during groundwater remediation. *J. Contam. Hydrol.* **2015**, in press; DOI: 10.1016/j.jconhyd.2015.03.004.
(36) Shi, Z.; Nurmi, J. T.; Tratnyek, P. G. Effects of nano zero-valent iron (nZVI) on oxidation-reduction potential (ORP). *Environ. Sci. Technol.* **2011**, *45*, 1586−1592.
(37) Field, J. A.; Reed, R. L.; Istok, J. D.; Semprini, L.; Bennett, P.; Buscheck, T. E. Trichlorofluoroethene: a reactive tracer for evaluating reductive dechlorination in large-diameter permeable columns. *Groundwater Monit. Rem.* **2005**, *25*, 68−77.
(38) Tratnyek, P. G.; Reilkoff, T. E.; Lemon, A. W.; Scherer, M. M.; Balko, B. A.; Feik, L. M.; Henegar, B. D. Visualizing redox chemistry: Probing environmental oxidation-reduction reactions with indicator dyes. *Chem. Educ.* **2001**, *6*, 172−179.
(39) Jones, B. D.; Ingle, J. D., Jr Evaluation of immobilized redox indicators as reversible, in situ redox sensors for determining Fe(III)-reducing conditions in environmental samples. *Talanta* **2001**, *55*, 699−714.
(40) Jones, B. D.; Ingle, J. D., Jr Evaluation of redox indicators for determining sulfate-reducing and dechlorinating conditions. *Water Res.* **2005**, *39*, 4343−4354.
(41) O'Loughlin, E. J. Effects of electron transfer mediators on the bioreduction of lepidocrocite (γ-FeOOH) by *Shewanella putrefaciens* CN32. *Environ. Sci. Technol.* **2008**, *42*, 6876−6882.
(42) Zhang, H.; Colón, D.; Kenneke, J. F.; Weber, E. J. The use of chemical probes for the characterization of the predominant abiotic reductants in anaerobic sediments. In *Aquatic Redox Chemistry*; Tratnyek, P. G., Grundl, T. J., Haderlein, S. B., Eds.; American Chemical Society: Washington, DC, 2011; ACS Symposium Series, Vol. *1071*; pp 539−557.
(43) Royer, R. A.; Burgos, W. D.; Fisher, A. S.; Unz, R. F.; Dempsey, B. A. Enhancement of biological reduction of hematite by electron shuttling and Fe(II) complexation. *Environ. Sci. Technol.* **2002**, *36*, 1939−1946.
(44) Tratnyek, P. G.; Wolfe, N. L. Characterization of the reducing properties of anaerobic sediment slurries using redox indicators. *Environ. Toxicol. Chem.* **1990**, *9*, 289−295.
(45) Clark, W. M. *Oxidation-Reduction Potentials of Organic Systems*; Williams & Wilkins: Baltimore, 1960.
(46) Bishop, E. *Indicators*; Pergamon: Oxford, 1972.
(47) Glavee, G. N.; Klabunde, K. J.; Sorensen, C. M.; Hadjipanayis, G. C. Chemistry of borohydride reduction of iron(II) and iron(III) ions in aqueous and nonaqueous media. Formation of nanoscale Fe, FeB, and Fe2B powders. *Inorg. Chem.* **1995**, *34*, 28−35.
(48) Orsetti, S.; Laskov, C.; Haderlein, S. B. Electron transfer between iron minerals and quinones: Estimating the reduction potential of the Fe(II)-goethite surface from AQDS speciation. *Environ. Sci. Technol.* **2013**, *47*, 14161−14168.
(49) Baer, D. R.; Grosz, A. E.; Ilton, E. S.; Krupka, K. M.; Liu, J.; Penn, R. L.; Pepin, A. Separation, characterization and initial reaction studies of magnetite particles from Hanford sediments. *Physics and Chemistry of the Earth* **2010**, *35*, 233−241.
(50) Mahmoodlu, M. G.; Hassanizadeh, S. M.; Hartog, N. Evaluation of the kinetic oxidation of aqueous volatile organic compounds by permanganate. *Sci. Total Environ.* **2014**, *485−486*, 755−763.
(51) Tratnyek, P. G. Comment on "Evaluation of the kinetic oxidation of aqueous volatile organic compounds by permanganate" by M. G. Mahmoodlu, S. M. Hassanizadeh, and N. Hartog, in Science of the Total Environment (2014) 485−486: 755−763. *Sci. Total Environ.* **2015**, *502*, 722−723.
(52) Shi, Z.; Zachara, J. M.; Shi, L.; Wang, Z.; Moore, D. A.; Kennedy, D. W.; Fredrickson, J. K. Redox reactions of reduced flavin mononucleotide (FMN), riboflavin (RBF), and anthraquinone-2,6-

DOI: 10.1021/acs.est.5b02804
Environ. Sci. Technol. 2015, 49, 10589−10597

disulfonate (AQDS) with ferrihydrite and lepidocrocite. *Environ. Sci. Technol.* **2012**, *46*, 11644−11652.
(53) Liu, T.; Li, X.; Waite, T. D. Depassivation of aged Fe^0 by ferrous ions: Implications to contaminant degradation. *Environ. Sci. Technol.* **2013**, *47*, 13712−13720.
(54) Huang, Y. H.; Zhang, T. C. Effects of dissolved oxygen on formation of corrosion products and concomitant oxygen and nitrate reduction in zero-valent iron systems with or without aqueous Fe^{2+}. *Water Res.* **2005**, *39*, 1751−1760.
(55) Reardon, E. J. Zerovalent irons: Styles of corrosion and inorganic control on hydrogen pressure buildup. *Environ. Sci. Technol.* **2005**, *39*, 7311−7317.
(56) Velimirovic, M.; Carniato, L.; Simons, Q.; Schoups, G.; Seuntjens, P.; Bastiaens, L. Corrosion rate estimations of microscale zerovalent iron particles via direct hydrogen production measurements. *J. Hazard. Mater.* **2014**, *270*, 18−26.
(57) Paar, H.; Ruhl, A. S.; Jekel, M. Influences of nanoscale zero valent iron loadings and bicarbonate and calcium concentrations on hydrogen evolution in anaerobic column experiments. *Water Res.* **2015**, *68*, 731−739.
(58) Filip, J.; Karlický, F.; Marušák, Z.; Lazar, P.; Černík, M.; Otyepka, M.; Zbořil, R. Anaerobic reaction of nanoscale zerovalent iron with water: Mechanism and kinetics. *J. Phys. Chem. C* **2014**, *118*, 13817−13825.
(59) Kocur, C. M.; Chowdhury, A. I.; Sakulchaicharoen, N.; Boparai, H. K.; Weber, K. P.; Sharma, P.; Krol, M. M.; Austrins, L.; Peace, C.; Sleep, B. E.; O'Carroll, D. M. Characterization of nZVI mobility in a field scale test. *Environ. Sci. Technol.* **2014**, *48*, 2862−2869.
(60) Miehr, R.; Tratnyek, P. G.; Bandstra, J. Z.; Scherer, M. M.; Alowitz, M.; Bylaska, E. J. The diversity of contaminant reduction reactions by zero-valent iron: Role of the reductate. *Environ. Sci. Technol.* **2004**, *38*, 139−147.
(61) Schöftner, P.; Waldner, G.; Lottermoser, W.; Stöger-Pollach, M.; Freitag, P.; Reichenauer, T. G. Electron efficiency of nZVI does not change with variation of environmental parameters. *Sci. Total Environ.* **2015**, in press; DOI: 10.1016/j.scitotenv.2015.05.033.

DOI: 10.1021/acs.est.5b02804
Environ. Sci. Technol. 2015, 49, 10589−10597